



Triggering of major eruptions recorded by actively forming cumulates

Michael J. Stock*, Rex N. Taylor & Thomas M. Gernon

National Oceanography Centre, Southampton, University of Southampton, Southampton SO14 3ZH, U.K.

SUBJECT AREAS:

GEOCHEMISTRY

PETROLOGY

SOLID EARTH SCIENCES

VOLCANOLOGY

Received

15 August 2012

Accepted

17 September 2012

Published

12 October 2012

Correspondence and requests for materials should be addressed to

R.N.T. (rex@noc.soton.ac.uk)

* Current address:

Department of Earth Sciences, Oxford OX1 3AN, U.K.

Major overturn within a magma chamber can bring together felsic and mafic magmas, prompting de-volatilisation and acting as the driver for Plinian eruptions. Until now identification of mixing has been limited to analysis of lavas or individual crystals ejected during eruptions. We have recovered partially developed cumulate material ('live' cumulate mush) from pyroclastic deposits of major eruptions on Tenerife. These samples represent "frozen" clumps of diverse crystalline deposits from all levels in the developing reservoir, which are permeated with the final magma immediately before eruptions. Such events therefore record the complete disintegration of the magma chamber, leading to caldera collapse. Chemical variation across developing cumulus crystals records changes in melt composition. Apart from fluctuations reflecting periodic influxes of mafic melt, crystal edges consistently record the presence of more felsic magmas. The prevalence of this felsic liquid implies it was able to infiltrate the entire cumulate pile immediately before each eruption.

The Las Cañadas volcano on Tenerife, Canary Islands, generated at least seven major explosive eruptions during the Quaternary^{1–3}. These events resulted in widespread deposition of pyroclastic material, with an estimated volume of >130 km³ (ref. 1,4). Despite considerable scientific interest in the volcano and associated hazards including major landslides⁵, little is known about the triggers for these large-scale events⁶. Early eruptions (~2 Ma) involved the explosive ejection of large volumes of phonolite magma, implosion of the volcanic edifice and development of the 16 km wide Las Cañadas caldera¹. Products of this explosive phase are preserved within the caldera wall and the extensive pyroclastic apron of the Bandas del Sur (Fig. 1). More than seven ignimbrite units occur within the apron, each recording a separate Plinian eruption that culminated in a caldera collapse event¹. Trachytes and phonolites of the Teide-Pico Viejo complex provide evidence that felsic magma remains beneath the centre of Tenerife^{3,5}.

We have identified crystal cumulate nodules in ignimbrites from three major explosive eruptions: Fasnía, Poris and La Caleta¹. Their distribution is laterally and stratigraphically variable within ignimbrite units, likely as a result of complex pyroclastic processes. These cumulates were not completely solidified before each eruption, and retain layers containing abundant inter-cumulus melt <1 cm thick. Similar examples of crystal mush have been recorded from other effusive⁷ and explosive⁸ eruptions. However, here we use the 'live' cumulate nodules from Tenerife as a tool to examine the repeating magmatic processes that occurred prior to explosive volcanic eruptions. We present major and trace element chemical profiles across cumulate crystals to examine the magmatic processes that occurred during the development of the compositionally stratified magma chamber⁹, particularly during the final stages prior to eruption^{10,11}.

Each of the mafic nodules contains medium-coarse grained cumulate crystals that are either in grain boundary contact as an adcumulate texture, or are partially separated by layers or domains rich in a microcrystalline, glassy groundmass. These melt-rich domains are bounded by crystalline layers and are quenched upon ejection from the magma chamber. As such, these nodules trap and have preserved the final liquid in contact with the cumulate which was actively forming at the margins of the magma chamber. It is the presence of discrete layers containing up to 80% interstitial melt that sets these apart from regular cumulates.

The most mafic nodules are wherlites, taken to represent material close to the chamber floor. Successively higher layers in the system are represented by gabbro, hornblende gabbro and foid gabbro to syenite. Within the gabbroic nodules, plagioclase (An_{50–88}) is more primitive (mafic) than individual crystals in juvenile pumice from the same eruption⁶. Well-defined core regions occur within many cumulus plagioclases and are overgrown by oscillatory or simple zoned mantles, occasionally with well-developed sieve textures. Clinopyroxene compositions are comparatively limited, ranging En_{31–42}Fs_{12–19}Wo_{46–50}, similar to, or slightly more Mg-rich, than those in juvenile pumice⁶. Typically, they have defined cores, with multiple and oscillatory zoned overgrowth mantles. Grain boundaries are generally well preserved, particularly in layers where the cumulus phases are separated by

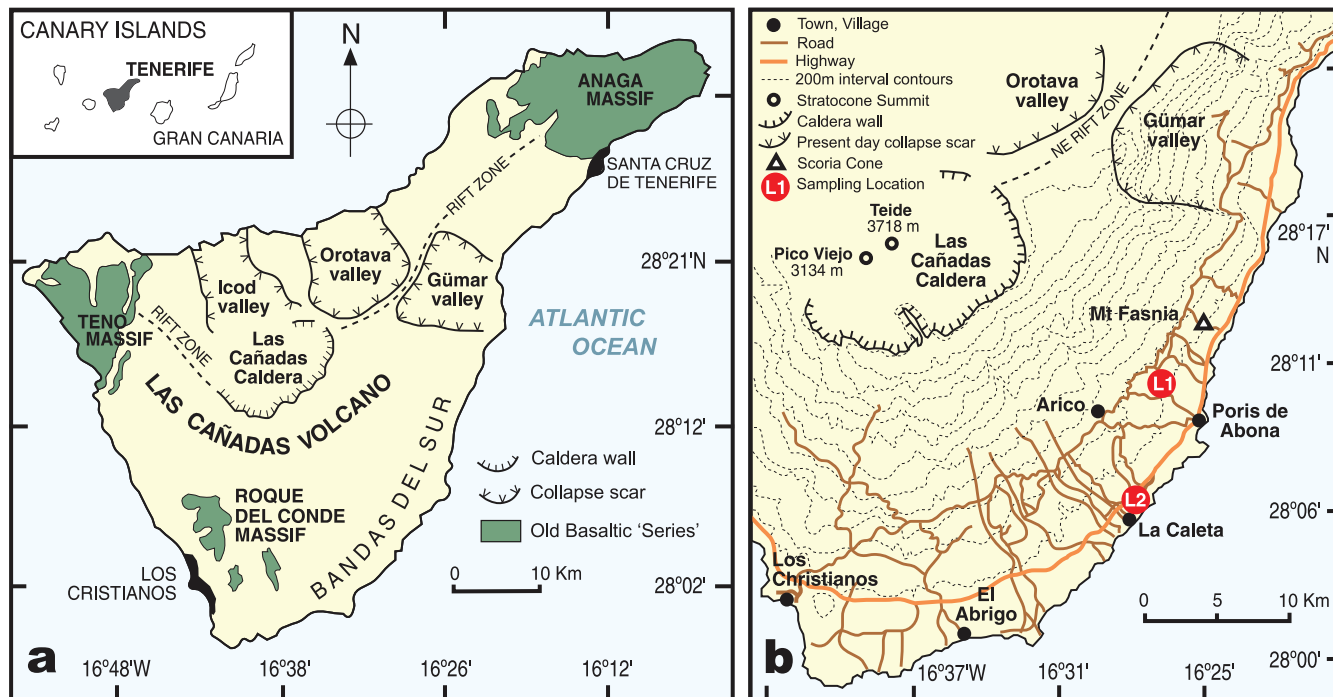


Figure 1 | Map of Tenerife showing locations of sampling sites. (a) Regional map of Tenerife showing major geological features and the location of the Bands del Sur pyroclastic apron. Inset shows the position of Tenerife within the Canary Islands. (b) Detailed map of the Bands del Sur Region, with sampling locations shown (modified after Ref. 1).

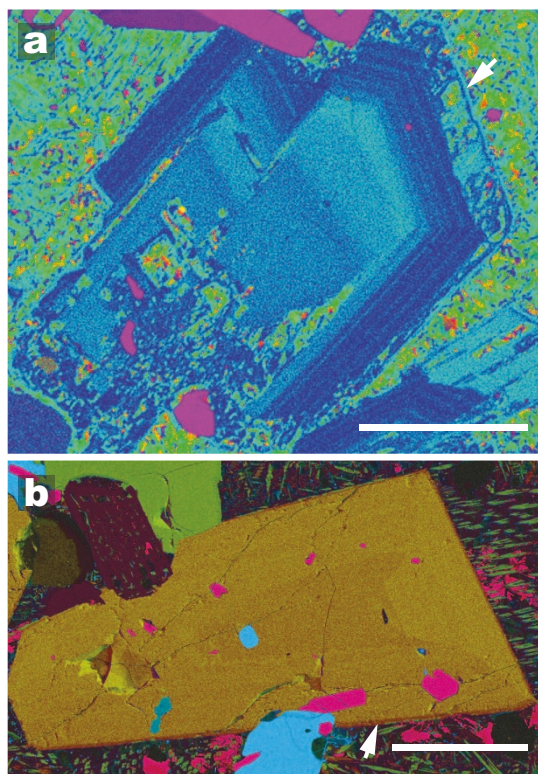


Figure 2 | Three-component electron microprobe element maps of zoned cumulus phases. (a) Variation in Na:Ca:K across a plagioclase cumulus crystal from the La Caleta Formation; note that lighter blue colours represent more albitic compositions. (b) Variation in Mg:Fe:Ca across a clinopyroxene cumulus crystal from the Fasnía Formation; note that darker orange colours represent more Fe-rich compositions. Colours are qualitative within each image and cannot be compared. Arrows highlight evolved rim zones at the crystal exteriors. Scale bar is 500 μm on both images.

regions of interstitial melt. A key feature of both the plagioclase and clinopyroxenes adjacent to this melt is a thin, optically bright zone ($<40 \mu\text{m}$ wide) at the crystal rim (Fig. 2).

Results

Major element concentrations of minerals vary in response to both melt composition and magma chamber conditions including pressure, temperature, volatile content and oxygen fugacity ($f\text{O}_2$)¹². However, trace element concentrations are almost entirely a function of melt composition and are largely independent of changes in intensive parameters¹¹. With the exception of rare patchy crystals, concentric zonation is evident (Fig. 2), implying little alteration by post-crystallization diffusion¹². Within crystal mantles, compositions oscillate (Fig. 3), but zonation generally shows increasing An# ($\text{Ca}/(\text{Ca}+\text{Na}) \times 100$) in plagioclase, and either flat or slightly increasing Mg# ($\text{Mg}/(\text{Mg}+\text{Fe}) \times 100$) in clinopyroxene towards the outer rim (i.e. reverse zoning). This is also reflected in trace element transects by increasing FeO in plagioclase (Fig. 3). However, the most striking feature of the cumulus zoning is a sharp decrease in plagioclase An# and clinopyroxene Mg# at the rims of these crystals, with a corresponding drop in Fe content and Al/Ti over the same distance.

In plagioclase, An# correlates positively with melt temperature and H_2O content, with changes in chamber pressure exerting only a minor control¹³. Additionally, fluctuations in clinopyroxene Mg# can occur in response to changes in melt $f\text{O}_2$ (Ref. 14). Therefore, the oscillatory major element zoning may result from closed system processes, including crystal movement along thermal or compositional gradients, or open system processes, such as magmatic recharge^{11,13}. However, the large magnitude changes in An# and Mg# approaching the rim of the cumulate minerals are unlikely to result from variations in intensive parameters alone¹², and are more consistent with a sudden switch to a more evolved (felsic) melt composition.

As a trace element in plagioclase, Sr correlates negatively with An# through the crystal mantles (Fig. 3). Although bulk melt composition may influence plagioclase-melt Sr partitioning, particularly in more evolved systems^{10,13}, the dominant control on Sr is its increasing

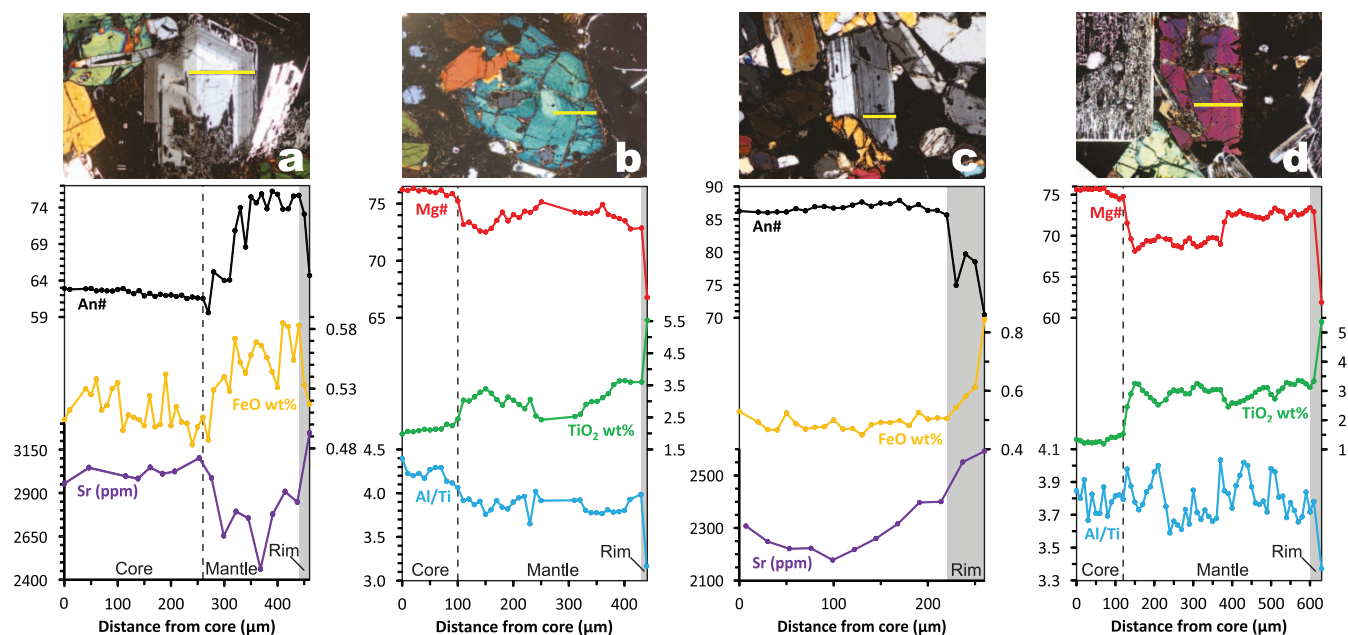


Figure 3 | Compositional profiles across representative plagioclase and clinopyroxene cumulus phases. (a) plagioclase and (b) clinopyroxene crystals from the La Caleta Formation, (c) plagioclase crystal from the Poris Formation, (d) clinopyroxene crystal from the Fasnja Formation. Photomicrograph images above the compositional profiles show optical zoning and position of compositional transects, shown below, which were collected from core to rim. The boundary between core- and mantle-regions is shown with a dashed line, where applicable. The grey shading in compositional profiles highlights the evolved zone at the crystal rims.

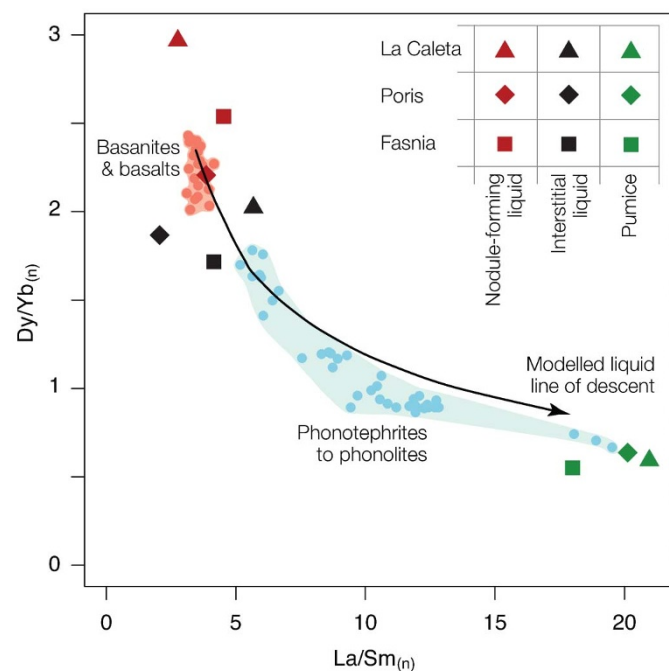


Figure 4 | Chondrite normalised rare earth element systematics of the Las Cañadas volcanics. Rare earth data are shown for: 1. Nodule forming liquids (calculated to be in equilibrium with the bulk cumulus phases, excluding rim), 2. Groundmass material, representing the final interstitial liquid, and 3. Juvenile pumice. Each of these categories was measured for the La Caleta, Poris and Fasnja Formations. For comparison, Tenerifean basanites-basalts and phonotephrites-phonolites are plotted as the pink and blue data fields respectively. Evolution of Tenerifean liquids is shown as the black line. All data were normalised using the C1 chondrite in ref. 38. Details of the data sources and modelling are presented in the methods section.

compatibility in plagioclase with decreasing An#¹⁵. Thus, the observed Sr zonation pattern is predicted by its changing partition coefficient, in response to this crystal-chemical control. In contrast, melt composition has the greatest effect on plagioclase Fe content¹³. This is known to increase with melt fO_2 (ref. 16) and correlates negatively with temperature and An#^{13,17}. However, within the oscillatory zoned plagioclase mantles, An# correlates positively with FeO (Fig. 3). As such, An-content and temperature may not have had a large influence on the Fe content of plagioclase. fO_2 -induced variations in plagioclase-liquid Fe partitioning are also unlikely to have significantly influenced Fe zoning, as this can not simply result in the positive correlation between An# and FeO. Variations in FeO are more readily explained by changes in melt composition resulting from repeated recharge of the fractionating magma chamber.

Variation in Al/Ti is a useful indicator of melt evolution in Cr-deficient clinopyroxene crystals¹⁸. While Al and Ti concentrations may be affected by temperature, pressure and rate of crystal growth¹⁹, the Al/Ti ratio more strongly reflects changes in melt composition¹⁴. A minor increase in clinopyroxene Al/Ti with temperature may occur due to the stronger partitioning of both Al^{IV} and Al^{VII}. Although temperature fluctuations could cause the positive correlation between Al/Ti and Mg# observed within oscillatory zoned clinopyroxene mantles (Fig. 3), Ti concentration also shows a well-defined anticorrelation with Mg#, which cannot result from variations in temperature alone¹⁹. Variable pressure is also an unlikely explanation for oscillatory Al/Ti zoning, as closed system convection would only cause small pressure changes (<1 kb)²⁰. Increased crystal growth rates relate to the degree of undercooling and correlate positively with Al and Ti²¹. This could explain the anti-correlation between Ti concentration and Mg#, so increased growth rates cannot be fully discounted as the cause of chemical Al/Ti zonation. However, all the clinopyroxenes exhibit concentric, rather than hourglass zoning, which would be expected if growth rate strongly influenced chemical zonation²¹. As such, clinopyroxene trace element zoning more likely records changes in melt composition.

Concordance of the plagioclase and clinopyroxene zoning patterns through the mantles of the cumulate phases is found in each

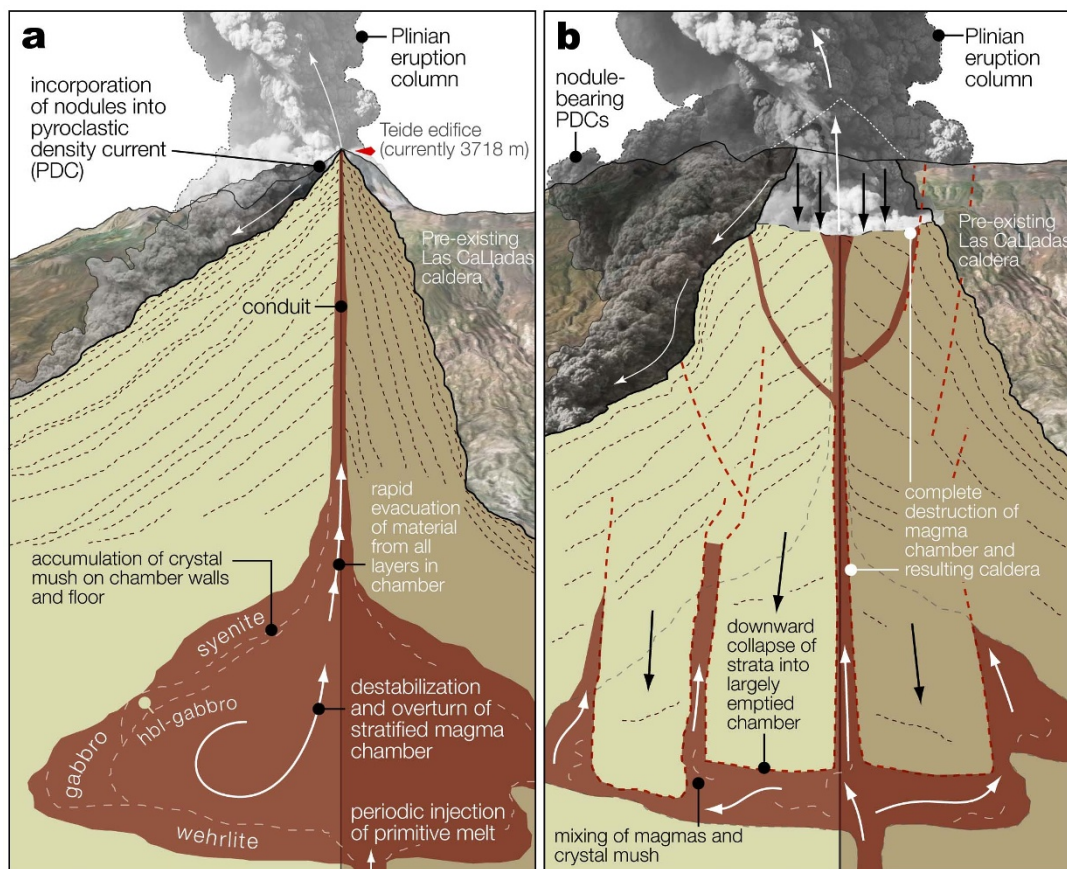


Figure 5 | Schematic diagram showing the repeating development of the Las Cañadas magma chamber. (a) Explosive eruption of the Las Cañadas volcano is triggered by destabilisation of the stratified magma chamber. (b) Incorporation of nodules from all magma chamber units into major pyroclastic density currents¹ and resulting caldera collapse.

of the ignimbrite units. This is consistent with a fractionating magma chamber, periodically refilled by more primitive melt, rather than fluctuations in parameters such as pressure and temperature (e.g. refs. 22, 23). Petrological evidence, such as sieve textured plagioclase phenocrysts, compositionally distinct phenocryst cores and overgrowth mantles also suggest that open system mixing occurred during chamber development²⁴. However, elemental oscillations cannot be correlated between crystals, indicating these events did not affect the whole chamber equally.

Changes in trace element concentrations accompany major element variations observed at crystal rims. In one plagioclase (La Caleta), the drop in An# at the rim correlates with a substantial ($\leq 11\%$) decrease in FeO concentration. This suggests that the rim zone reflects a significant change in melt composition, with lower FeO and An# indicative of crystallisation from a more evolved liquid. In contrast, rim zones in other plagioclase crystals from the three ignimbrites show an increase in FeO concentration, mirroring the drop in An#. This can be explained by cooling and rapid crystal growth, potentially accompanied by an increase in melt fO_2 , associated with a change to more evolved melt compositions. During rapid crystal growth, a chemical boundary layer, enriched in plagioclase incompatible elements such as Fe, may form at the crystal-melt interface¹³. Although such kinetic effects could contribute to the high Fe concentrations at crystal rims, they cannot account for the concurrent drop in An#. Contrasting Fe enrichment and depletion trends observed within rims of different plagioclase crystals are likely to result from varying degrees of undercooling. Both require a significant change in melt composition, regardless of the concentration shift direction. A large drop in Al/Ti accompanies the decrease in Mg# at the rim of most clinopyroxene phenocrysts analysed in this

study and is taken as a further indication of a large-scale change in melt chemistry.

To test if the interstitial melt is in equilibrium with Tenerifian basaltic liquids or more evolved phonolitic compositions, we recovered and analysed interstitial material from nodules in each unit. Figure 4 shows that these interstices are displaced towards more phonolitic compositions relative to the liquids in equilibrium with the cumulus crystal-forming melts (excluding rims). As such, the “frozen” final liquids within these cumulates confirm that mixing occurred between phonolitic and basaltic magmas before each eruption.

Discussion

Rim zones are thin ($<40 \mu\text{m}$), thus final growth is likely to represent only a brief period prior to eruption, probably on the order of 7–132 days²⁵. Low An# and Mg# in these rims suggests final growth in the presence of a significantly more evolved liquid, and the sharpness of this change precludes normal fractional crystallization. This is supported by the presence of an intercumulus liquid within the final “frozen” nodule, which has a more evolved composition than the liquid from which the cumulus phases crystallised. Two scenarios could explain the observed zonation: (1) The magma chamber was recharged with felsic melt, sourced from a separate, more evolved chamber. This has been recorded elsewhere²⁶ but on Tenerife would require a third magma reservoir, separate to the Las Cañadas chamber and the source of mafic recharge magma; or (2) The stratified magma chamber became destabilised, causing mixing between evolved material close to the chamber roof with primitive material at the base (Fig. 5)²⁷. Such an overturn may be driven by heating at the base of the magma chamber²⁸, sinking of cold, dense plumes from an



upper cupola layer¹⁰ or cooling and de-volatilisation of mafic magma close to the boundary with the overlying felsic material causing a density decrease²⁹. Pre-eruptive mixing scenarios are supported by the presence of banded pumice within each formation¹.

Similar evolved rims have been identified within phenocrysts from Tenerifian lavas, and these have been related to overturn of a stratified magma chamber¹⁰. The lack of any well-defined resorption surface between the rim and mantle suggests rim growth did not involve a significant change in magmatic temperature, so the eruption cannot easily be explained by felsic recharge¹⁰. Cumulate crystals analysed in this study also lack a clear resorption surface between the oscillatory mantle and rim zone and testify to a similar overturn-mixing scenario. Furthermore, there is a lack of evidence for two substantial, high-level, evolved magma chambers coexisting between Plinian eruptions.

Multiple Plinian eruptions punctuated the volcanic development of Tenerife through the Quaternary, separated by quiescent periods ranging between 10 ka and 300 ka. Approximately 170 ka has elapsed since the last Plinian eruption, but this may be irrelevant if magmatic systems can reach critical eruptive states within decades³⁰. Regardless of the timescales, the pre-climactic phase of magma chamber development appears to be consistent and systematic. Large-scale felsic-mafic magma interaction, preserved in partially developed crystal cumulates, appears to be the repeating trigger for destruction of the Las Cañadas magma chamber.

Methods

Electron microprobe analysis. Mineral major element compositions, plagioclase FeO and clinopyroxene TiO₂ and Al₂O₃ concentrations were determined using a Cameca SX-100 five spectrometer electron microprobe in Earth and Environmental Science at the Open University, operating in wavelength-dispersion mode. All analyses were collected using a 20 kV accelerating voltage and 20 nA beam current. Measurements were made along a linear transect outwards from the crystal cores, with a 10 μm beam diameter. Count times range between 20 and 80s per element. Calibration standards include: jadeite (Na), bustamite (Ca), hematite (Fe), forsterite (Mg), K-feldspar (Al) and rutile (Ti). Relative reproducibility estimates (2 sd) obtained from repeat analysis of a kaersutite reference material are $\leq \pm 1\%$ (CaO), $\leq \pm 2\%$ (MgO, FeO, Al₂O₃), $\leq 3\%$ (TiO₂) and $\leq 5\%$ (Na₂O₃).

Solution ICP-MS analysis. Juvenile pumice and intercumulus material were analysed for trace elements by inductively coupled plasma-mass spectrometry (ICP-MS), using a Thermo X-series instrument in Ocean and Earth Science at the University of Southampton. Following HF and HNO₃ digestion, samples were diluted by 2000–4000 and introduced via a microconcentric nebuliser. REE ratio precision is estimated to be better than 2% relative (2 sd) based on repeat analyses of rock standard JB-2.

Laser ablation ICP-MS analysis. Plagioclase Sr and clinopyroxene REE concentrations were determined using a Thermo X-Series II ICP-MS interfaced with a New Wave 193 excimer laser ablation system in Ocean and Earth Science at the University of Southampton. Typically measurements were conducted using a 5 Hz laser repetition rate with an 85% output. Count times were 20s and an Ar carrier gas was used. Data were collected along linear transects, equivalent to the previous microprobe measurements, using a 20 μm laser spot size, with a 3 μm bridge between analyses. ICP-MS results were calibrated using NIST 610 and NIST 614 reference glasses. Relative reproducibility estimates for Sr, La, Sm, Dy and Yb are ± 3 –4% (2 sd).

Data were excluded from both microprobe and LA-ICP-MS transects where analyses sampled inclusions or cracks within crystals. Additionally, points were discarded at the crystal rims where results showed evidence for any incorporation of intercumulus material.

Crystal fractionation modeling. A liquid evolution curve for the Tenerife alkaline magmas was calculated using a starting composition of basaltic lava DH97-28A³¹. Liquids were calculated using the modal assemblages of basaltic, phonotephrite and phonolite lavas of Ablay et al.³² and the partition coefficients of Fujimaki et al.³³, Fujimaki³⁴, Neuman³⁵, and Nielsen et al.³⁶. An initial 60% crystallisation used an assemblage with modal fractions olivine: clinopyroxene: magnetite: apatite = 0.296: 0.561: 0.006: 0.115: 0.012. The final liquid of this stage was then crystallised by a further 40% using olivine: clinopyroxene: plagioclase: magnetite: apatite = 0.050: 0.589: 0.198: 0.146: 0.016. Subsequently, this liquid was crystallised by 50% using olivine: clinopyroxene: plagioclase: amphibole: magnetite: apatite = 0.016: 0.190: 0.334: 0.295: 0.138: 0.047.

Data sources for Las Cañadas volcanics. For comparison with our measured data we have compiled rare earth element data for the Las Cañadas volcanics (Fig. 4),

throughout the explosive phase of Tenerifian development. Samples include lavas, dykes and explosive ejecta which were sourced from the Bandas del Sur region and the Las Cañadas caldera wall. They are grouped according to their major element composition (i.e. primitive and evolved). Data sources are as follows:

Basalts and basanites: data sourced from ref. 6,23,31

Phonotephrites to phonolites: data sourced from ref. 23,31,37

- Brown, R. J., Barry, T. L., Branney, M. J., Pringle, M. S. & Bryan, S. E. The Quaternary pyroclastic succession of southeast Tenerife, Canary Islands: explosive eruptions, related caldera subsidence, and sector collapse. *Geological Magazine* **140**, 265–288 (2003).
- Bryan, S. E., Martí, J. & Cas, R. Stratigraphy of the Bandas del Sur Formation: an extracaldera record of Quaternary phonolitic explosive eruptions from the Las Cañadas edifice, Tenerife (Canary Islands). *Geological Magazine* **135**, 605–636 (1998).
- Ancochea, E., Fuster, J., Ibarrola, E., Cendrero, A., Coello, J., Hernan, F., Cantagrel, J. M. & Jamond, C. Volcanic evolution of the island of Tenerife (Canary Islands) in the light of new K-Ar data. *Journal of Volcanology and Geothermal Research* **44**(3–4), 231–249 (1990).
- Martí, J., Mitjavila, J. & Araña, V. Stratigraphy, structure and geochronology of the Las Cañadas caldera (Tenerife, Canary Islands). *Geological Magazine* **131**(6), 715–727 (1994).
- Ablay, G. & Martí, J. Stratigraphy, structure, and volcanic evolution of the Pico Teide–Pico Viejo formation, Tenerife, Canary Islands. *Journal of Volcanology and Geothermal Research* **103**(1–4), 175–208 (2000).
- Bryan, S. E., Martí, J. & Leosson, M. Petrology and Geochemistry of the Bandas del Sur Formation, Las Cañadas Edifice, Tenerife (Canary Islands). *Journal of Petrology* **43**(10), 1815–1856 (2002).
- Holness, M. B. & Bunbury, J. M. Insights into continental rift-related magma chambers: Cognate nodules from the Kula Volcanic Province, Western Turkey. *Journal of Volcanology and Geothermal Research* **153**(3–4), 241–261 (2006).
- Tait, S. R., Wörner, G., Bogaard, P. V. D. & Schmincke, H.-U. Cumulate nodules as evidence for convective fractionation in a phonolite magma chamber. *Journal of Volcanology and Geothermal Research* **37**(1), 21–37 (1989).
- Wolff, J. A. Crystallisation of nepheline syenite in a subvolcanic magma system: Tenerife, canary islands. *Lithos* **20**(3), 207–223 (1987).
- Triebold, S., Kronz, A. & Wörner, G. Anorthite-calibrated backscattered electron profiles, trace elements, and growth textures in feldspars from the Teide–Pico Viejo volcanic complex (Tenerife). *Journal of Volcanology and Geothermal Research* **154**(1–2), 117–130 (2006).
- Rupprecht, P. & Wörner, G. Variable regimes in magma systems documented in plagioclase zoning patterns: El misti stratovolcano and andahua monogenetic cones. *Journal of Volcanology and Geothermal Research* **165**(3–4), 142–162 (2007).
- Streck, M. J. Mineral textures and zoning as evidence for open system processes. *Reviews in Mineralogy and Geochemistry* **69**(1), 595–622 (2008).
- Ginibre, C., Wörner, G. & Kronz, A. Minor- and trace-element zoning in plagioclase: implications for magma chamber processes at Paríacota volcano, northern Chile. *Contributions to Mineralogy and Petrology* **143**, 300–315 (2002). 10.1007/s00410-002-0351-z.
- Streck, M. J., Dungan, M. A., Malavassi, E., Reagan, M. K. & Bussy, F. The role of basalt replenishment in the generation of basaltic andesites of the ongoing activity at Arenal volcano, Costa Rica: evidence from clinopyroxene and spinel. *Bulletin of Volcanology* **64**, 316–327 (2002). 10.1007/s00445-002-0209-2.
- Blundy, J. D. & Wood, B. J. Crystal-chemical controls on the partitioning of sr and ba between plagioclase feldspar, silicate melts, and hydrothermal solutions. *Geochimica et Cosmochimica Acta* **55**(1), 193–209 (1991).
- Wilke, M. & Behrens, H. The dependence of the partitioning of iron and europium between plagioclase and hydrous tonalitic melt on oxygen fugacity. *Contributions to Mineralogy and Petrology* **137**, 102–114 (1999). 10.1007/s004100050585.
- Bindeman, I. N., Davis, A. M. & Drake, M. J. Ion microprobe study of plagioclase-basalt partition experiments at natural concentration levels of trace elements. *Geochimica et Cosmochimica Acta* **62**(7), 1175–1193 (1998).
- Streck, M. J., Dungan, M. A., Bussy, F. & Malavassi, E. Mineral inventory of continuously erupting basaltic andesites at Arenal volcano, Costa Rica: implications for interpreting monotonous, crystal-rich, mafic arc stratigraphies. *Journal of Volcanology and Geothermal Research* **140**(1–3), 133–155 (2005).
- Adam, J. & Green, T. The effects of pressure and temperature on the partitioning of Ti, Sr and REE between amphibole, clinopyroxene and basaltic melts. *Chemical Geology* **117**(1–4), 219–233 (1994).
- Ginibre, C., Kronz, A. & Wörner, G. High-resolution quantitative imaging of plagioclase composition using accumulated backscattered electron images: new constraints on oscillatory zoning. *Contributions to Mineralogy and Petrology* **142**, 436–448 (2002). 10.1007/s004100100298.
- Skulski, T., Minarik, W. & Watson, E. B. High-pressure experimental trace-element partitioning between clinopyroxene and basaltic melts. *Chemical Geology* **117**(1–4), 127–147 (1994).
- O'Hara, M. J. Geochemical evolution during fractional crystallisation of a periodically refilled magma chamber. *Nature* **266**(5602), 503–507, 04 (1977).



23. Neumann, E.-R., Wulff-Pedersen, E., Simonsen, S. L., Pearson, N. J., Martí, J. & Mitjavila, J. Evidence for fractional crystallization of periodically refilled magma chambers in Tenerife, Canary Islands. *Journal of Petrology* **40**(7), 1089–1123 (1999).
24. Humphreys, M. C. S., Blundy, J. D. & Sparks, R. S. J. Magma evolution and open-system processes at Shiveluch Volcano: Insights from phenocryst zoning. *Journal of Petrology* **47**(12), 2303–2334 (2006).
25. Larsen, J. F. Experimental study of plagioclase rim growth around anorthite seed crystals in rhyodacitic melt. *American Mineralogist* **90**(2-3), 417–427 (2005).
26. de Silva, S., Salas, G. & Schubring, S. Triggering explosive eruptions—The case for silicic magma recharge at Huaynaputina, southern Peru. *Geology* **36**, 387–390 (2008).
27. Sparks, S. R. J., Sigurdsson, H. & Wilson, L. Magma mixing: a mechanism for triggering acid explosive eruptions. *Nature* **267**, 315–318 (1977).
28. Couch, S., Sparks, R. S. J. & Carroll, M. R. Mineral disequilibrium in lavas explained by convective self-mixing in open magma chambers. *Nature* **411**, 1037–1039 (2001).
29. Huppert, H. E., Sparks, R. S. J. & Turner, J. S. Effects of volatiles on mixing in calc-alkaline magma systems. *Nature* **297**(5867), 554–557 (1982).
30. Druitt, T. H., Costa, F., Delouie, E., Dungan, M. & Scaillet, B. Decadal to monthly timescales of magma transfer and reservoir growth at a caldera volcano. *Nature* **482**(7383), 77–80 (2012).
31. Wolff, J., Grandy, J. & Larson, P. Interaction of mantle-derived magma with island crust? Trace element and oxygen isotope data from the Diego Hernandez Formation, Las Cañadas, Tenerife. *Journal of Volcanology and Geothermal Research* **103**(1–4), 343–366 (2000).
32. Ablay, G. J., Carroll, M. R., Palmer, M. R., Martí, J. & Sparks, R. S. J. Basanite–phonolite lineages of the Teide–Pico Viejo Volcanic Complex, Tenerife, Canary Islands. *Journal of Petrology* **39**(5), 905–936 (1998).
33. Fujimaki, H., Tatsumoto, M. & Aoki, K.-i. Partition coefficients of Hf, Zr, and REE between phenocrysts and groundmasses. *J. Geophys. Res.* **89**(S2), B662–B672 (1984).
34. Fujimaki, H. Partition coefficients of Hf, Zr, and REE between zircon, apatite, and liquid. *Contributions to Mineralogy and Petrology* **94**, 42–45 (1986). 10.1007/BF00371224.
35. Neumann, E.-R., Wulff-Pedersen, E., Pearson, N. J. & Spencer, E. A. Mantle xenoliths from Tenerife (Canary Islands): Evidence for reactions between mantle peridotites and silicic carbonatite melts inducing ca metasomatism. *Journal of Petrology* **43**(5), 825–857 (2002).
36. Nielsen, R. L., Gallahan, W. E. & Newberger, F. Experimentally determined mineral-melt partition coefficients for Sc, Y and REE for olivine, orthopyroxene, pigeonite, magnetite and ilmenite. *Contributions to Mineralogy and Petrology* **110**, 488–499 (1992). 10.1007/BF00344083.
37. Bryan, S. E. Petrology and geochemistry of the Quaternary caldera-forming, phonolitic Granadilla Eruption, Tenerife (Canary Islands). *Journal of Petrology* **47**(8), 1557–1589 (2006).
38. Sun, S.-s. & McDonough, W. F. Chemical and isotopic systematics of oceanic basalts: implications for mantle composition and processes. *Geological Society, London, Special Publications* **42**(1), 313–345 (1989).

Acknowledgements

We are grateful to A. Milton and A. Tindle for their assistance with the ICP-MS and microprobe respectively. We thank J. Blundy and M. Lane for helpful discussions, and acknowledge M. Cassidy for providing field assistance. K. Davis is thanked for drafting the maps shown in Figure 1.

Author contributions

R.T. directed the research; M.S., R.T. and T.G. carried out the fieldwork and sampling; M.S. and R.T. carried out the analytical work and modelling. All authors wrote the paper, drafted the figures, discussed the results and contributed to the final manuscript.

Additional information

Competing financial interests: The authors declare no competing financial interests.

License: This work is licensed under a Creative Commons Attribution-NonCommercial-NoDerivative Works 3.0 Unported License. To view a copy of this license, visit <http://creativecommons.org/licenses/by-nc-nd/3.0/>

How to cite this article: Stock, M.J., Taylor, R.N. & Gernon, T.M. Triggering of major eruptions recorded by actively forming cumulates. *Sci. Rep.* **2**, 731; DOI:10.1038/srep00731 (2012).



DOI: 10.1038/srep01589

SUBJECT AREAS:

GEOCHEMISTRY

PETROLOGY

VOLCANOLOGY

ENVIRONMENTAL SCIENCES

SCIENTIFIC REPORTS:

2 : 731

DOI: 10.1038/srep00731

(2012)

Published:

12 October 2012

Updated:

25 March 2013

ERRATUM: Triggering of major eruptions recorded by actively forming cumulates

Michael J. Stock, Rex N. Taylor & Thomas M. Gernon

Due to a technical error, the corresponding author is incorrectly given as Thomas M. Gernon rather than Rex N. Taylor in the HTML version of this Article. For correspondence and requests for materials, please contact Rex N. Taylor (rex@noc.soton.ac.uk). This error has now been updated in the original Article.